

Activation of TRPV4 channels reduces migration of immortalized neuroendocrine cells

Roberta Zaninetti,*¹ Alessandra Fornarelli,*¹ Monica Ciarletta,* Dmitry Lim,* Antonio Caldarelli,* Tracey Pirali,* Anna Cariboni,†,‡ Grzegorz Owsianik,§ Bernd Nilius,§ Pier Luigi Canonico,* Carla Distasi* and Armando A. Genazzani*

*Dipartimento di Scienze Chimiche, Alimentari, Farmaceutiche e Farmacologiche, Università degli Studi del Piemonte Orientale A. Avogadro, Novara, Italy

†Dipartimento di Endocrinologia, Fisiopatologia e Biologia Applicata, Università di Milano, Milano, Italy

‡Department of Cell and Developmental Biology, University College London, London, UK

§Department of Molecular Cell Biology, Laboratory of Ion Channel Research, KU Leuven, Leuven, Belgium

Abstract

Calcium is a universal signal, and its capacity to encode intracellular messages via spatial, temporal and amplitude characteristics allows it to participate in most cellular events. In a specific context, calcium plays a pivotal role in migration, although its role has not been elucidated fully. By using immortalized gonadotropin-releasing hormone-secreting neurons (GN11), we have now investigated the role of TRPV4, a member of the vanilloid family of Ca²⁺ channels, in neuronal migration. Our results show that TRPV4 channels are present

and functional in GN11 cells and their localization is polarized and enriched in lamellipodial structures. TRPV4 activation leads to a retraction of the lamellipodia and to a decrease in migratory behaviour; moreover cells migrate slower and in a more random manner. We therefore provide evidence for a new regulation of gonadotropin-releasing hormone neurons and a new role for calcium at the leading edge of migratory cells.

Keywords: calcium, gonadotropin-releasing hormone neurons, migration, TRPV4.

J. Neurochem. (2011) **116**, 606–615.

Developing gonadotropin-releasing hormone (GnRH) neurons originate in the nasal compartment and migrate in association with olfactory nerves (vomeronasal and terminal) to enter into the forebrain and reach their final destinations (Schwanzel-Fukuda and Pfaff 1989; Wray *et al.* 1989). The mechanisms underlying the establishment of the migration route and the movement of GnRH neurons are thought to involve different classes of molecules (for a review, see Tobet and Schwarting 2006). First of all, it is likely that transcriptional programs regulate the capacity and timing of GnRH neurons to migrate (Tobet and Schwarting 2006; Zaninetti *et al.* 2008; Orso *et al.* 2009). Secondly, it has been shown that a cohort of other pathways, including neurotransmitters, adhesion molecules, cell-cell interaction proteins, participate in the coordination of this migratory behaviour (Tobet and Schwarting 2006). It is likely that many of these molecules are necessary to generate gradients of attractant or to decode such gradients in the migrating GnRH-secreting neuron.

Calcium is a universal signal, and its capacity to encode intracellular messages via spatial, temporal and amplitude characteristics allows it to participate in most cellular events,

from egg fertilization to cell death, from neurotransmitter release to post-synaptic responses (Berridge 2001). In this view, it is not surprising that it has been heavily involved in neuronal motility, including migration (Zheng and Poo 2007). In GnRH neurons, it has been shown that calcium entry via N-type channels is essential for migration to occur (Toba *et al.* 2005). Furthermore, in a distinct setting, we have previously shown that the Ca²⁺/calineurin/nuclear factor of activated T-cells pathway is important to prime neurons for migration at the transcriptional level (Zaninetti *et al.* 2008). In other words, calcium appears to be important both for

Received June 10, 2010; revised manuscript received November 8, 2010; accepted December 10, 2010.

Address correspondence and reprint requests to Armando A Genazzani, DiSCAFF, Via Bovio, 6, 28100 Novara, Italy.

E-mail: genazzani@pharm.unipmn.it

¹These authors contributed equally.

Abbreviations used: 4 α -PDD, 4 α -phorbol 12,13 didecanoate; 4 α -PDH, 4 α -phorbol 12,13-dihexanoate; GnRH, gonadotropin-releasing hormone; FCS, fetal calf serum; GFP, green fluorescent protein; siRNA, small interfering RNA; TRP, transient receptor potential.

setting correct transcriptional programs and to execute migration itself.

Transient receptor potential (TRP) channels are a large family of heterogenous cation channels (Clapham *et al.* 2003; Nilius *et al.* 2007). The vanilloid subfamily (TRPV) is involved in sensing a number of diverse external and internal stimuli, including heat, osmotic stress, mechanic stress as well as chemical molecules (Vennekens *et al.* 2008; Vriens *et al.* 2009). TRPV4, which is permeable to calcium, is expressed in various tissues where it is involved in a number of physiological functions. Recently, it has been linked to a number of inherited diseases resulting from malfunction of the peripheral nervous system (reviewed in Nilius and Owsianik 2010).

In this work, we show that TRPV4 channels are present in GN11 cells, a well-established immortalized neuronal cell system that displays a migratory phenotype. As capsaicin-sensitive activation of TRPV1 and TRPV2, two close TRPV4 homologues, stimulate migration in liver carcinoma and prostate cells, respectively (Waning *et al.* 2007; Monet *et al.* 2010), we decided to investigate the role of TRPV4 in this context.

We now show that activation of TRPV4, which appears to be present on lamellipodia structures, inhibits neuronal migration, thereby providing evidence for a new regulation of GnRH neurons and, more broadly, for a new role of calcium at the leading edge of migratory cells.

Materials and methods

Cell cultures, animals, plasmids, transfection and sorting

GN11 and GT1–7 cells were originally provided by S. Radovick (University of Chicago, Chicago, IL, USA) and R. I. Weiner (San Francisco, CA, USA), respectively. The cells were grown in a monolayer at 37°C in a humidified CO₂ incubator in Dulbecco's modified Eagle's medium containing 1 mM sodium pyruvate, 2 mM glutamine, 100 µg/mL streptomycin, 100 U/mL penicillin and supplemented with 10% fetal calf serum (FCS). The medium was replaced at 2 day intervals. Subconfluent cells were routinely harvested by trypsinization and seeded in 10 cm diameter dishes.

Heads of embryos, removed from pregnant C57BL/6J mice or Sprague-Dawley albino rats at different stages of gestation [embryonic day 0 (E0) or 1 are the days when vaginal plug was respectively found] were used for RT-PCR. All animal procedures were performed in accordance with institutional guidelines.

For over-expression of TRPV4, GN11 cells were grown in culture plates in complete culture medium for 24 h and incubated for 3 h with the polycistronic expression vector containing internal ribosome entry site (IRES) followed by green fluorescent protein (GFP) TRPV4-IRES-GFP (Rock *et al.* 2008) in the presence of the LipofectamineTM-PlusTM Reagent (Invitrogen, Carlsbad, CA, USA) according to the manufacturer's instructions. Forty-eight hours after transfection cells were harvested by trypsinization and then resuspended (10×10^6 per mL) in phosphate-buffered saline (Ca/Mg²⁺-free) + 5 mM EDTA, 25 mM HEPES, pH 7.0 and 1% FCS and sorted in GFP⁺ and GFP⁻ populations using stringent conditions

to avoid cross-contaminations using a FACS Vantage SE (Becton-Dickinson, Franklin Lakes, NJ, USA).

To reduce TRPV4 expression, GN11 cells were plated on 10 cm diameter dishes (500 000 cells/plate) 12 h before transfection. Two microgram of small interfering RNA (siRNA) targeting TRPV4 (Applied Biosystems, Foster City, CA, USA; AGACAGTTCT CAACAATGATT) were incubated for 20 min at RT in Opti-MEM (200 µL; Invitrogen) and Lipofectamine 2000 (8 µL; Invitrogen), then added on top of the cells gently. Twelve hours after transfection, one volume of fresh medium was added. RNA depletion was assessed by real-time PCR 36 h after transfection. As a negative control, a pre-designed siRNA (Silencer[®] Select Negative Control #1 siRNA; Applied Biosystem) was used.

Microchemotaxis assay

The assay was performed using a 48-well Boyden's microchemotaxis chamber according to the instructions (Neuroprobe, Cabin John, MD, USA) as described previously (Zaninetti *et al.* 2008) and detailed in the Appendix S1.

Ca²⁺ measurements

Calcium imaging experiments were performed either with Fura-2 or with the transfected ratiometric fluorescence resonance energy transfer (FRET)-based sensor NT-XL (kindly provided by Dr Griesbeck; Mank *et al.* 2006). Experimental details are present in the Appendix S1.

Time-lapse video microscopy and cell migration analysis

Cells, plated at low density (100 000 cells/plate) on gelatin-coated 40 mm coverslips, were monitored using a phase-contrast optics in a Nikon Eclipse TE 300 microscope equipped with a heated (37°C) live cell closed chamber system (Biopetechs, Butler, PA, USA) connected to a peristaltic pump. Images were acquired with a cooled CCD camera (Sensicam; PCO, Kelheim, Germany) using the camera control software. Cell trajectory and other analysis were determined as the time sequence of the centroid position of the cell using a custom-made software written by SITEM, Italy. Full details of experimental procedures and data analysis are present in the Appendix S1.

Chemicals, antibodies and RT-PCR

5,6-Epoxyeicosatrienoic acid was purchased from Alexis Biochemicals, San Diego, CA, USA; 4 α -phorbol 12,13-dihexanoate (4 α -PDH) and 13-acetyl-12-tetradecanoyl-4 α -phorbol were kindly provided by Prof. G. Appendino; GSK1016790A, N-((1S)-1-1{[4-((2S)-2-{[2,4-dichlorophenyl]sulfonyl]amino}-3-hydroxyprop-1-yl)-1-piperazinyl]carbonyl}-3-methylbutyl)-1-benzothioephene-2-carboxamide, a substituted piperazine, was prepared in-house according to the GlaxoSmithKline (London, UK) patent WO 2007/070865 A2 (PCT/US2006/062147). Identity of the product was assessed by mass spectrometry and purity of the final product was assessed by NMR (1H and 13C) and was superior to 95%. All other chemicals were purchased from Sigma-Aldrich (St Louis, MO, USA).

The following antibodies were used: anti-TRPV4, rabbit polyclonal, Alomone labs and anti-TRPV4, rabbit polyclonal kindly provided by the laboratory of Bernd Nilius. Secondary was goat anti-rabbit Alexa Fluor 488 (Invitrogen).

For evaluation of *trpv4* transcript levels, a PCR approach (94°, 60°, 72°, 31 cycles) was used using primers detailed in the Appendix S1.

Purification of GFP-GnRH neurons from embryos and subsequent RNA extraction were performed as detailed in Cariboni *et al.* (2007).

Aggregates and wound healing

Cell aggregates were prepared by the ‘hanging drop’ technique as detailed in the Appendix S1. To perform wound healing experiments, cells were grown until subconfluent, the monolayer of cells was then scratched in way to create a cell-free corridor. Re-sealing was monitored for 16–18 h.

Statistical analysis

Data are presented as the mean values \pm SEM. One-way ANOVA followed by a statistical test for multiple comparisons (Origin, Tukey’s test) were applied to compare experimental treatments. The level of significance, unless indicated otherwise, was $p < 0.05$.

Results

TRPV4 is present and functional in GN11 cells

To establish whether *trpv4* transcript was present in GN11 cells, we performed an RT-PCR with primers that amplify regions corresponding to the N- or C-terminal part of the TRPV4 protein. Both sets of primers yielded a band of the expected size (Fig. 1a). Primers amplifying the N-terminal region also yielded a faint band of superior molecular weight, which might correspond to a splice variant but was not further characterized. In GT1–7 cells, the mature equivalent of GN11 cells that lack a migratory phenotype, *trpv4* was also present. GnRH neurons derive from the nasal placode and migrate

through the olfactory bulb. We therefore decided to probe whether *trpv4* transcript was present in mRNA extracted from these regions during embryonic development. Indeed, at E13 *trpv4* was enriched in the nasal area compared with the head without nose, and at E16 *trpv4* transcript was present both in the nasal area and in the encephalon (Fig. 1a). To further investigate the presence of *trpv4* in GnRH neurons we performed RT-PCR on mRNA of GFP-GnRH neurons isolated by fluorescence activated cell sorting (FACS) from transgenic mice (as described in Cariboni *et al.* 2007): a clear band was detected in such cells at E17 (Fig. 1b). In parallel, we also detected the presence of *trpv4* in embryonic rat tissue: using specific primers for the C-term form of rat TRPV4 in mRNA extracted from explants of olfactory bulbs and nasal tissue, we confirmed the presence of TRPV4 expression in those regions at E16 (Fig. 1c). Such patterns both in rat and mouse parallel the localization of GnRH neurons during development.

Using TRPV4 specific antibodies, we also confirmed the presence of TRPV4 bands (\sim 100 kDa) in homogenates from both GN11 and GT1–7 cells (Fig. 1d). A second higher immunoreactive band (around 110 kDa) might correspond to an alternative splice variant or to post-translational modifications of TRPV4. The specificity of these bands was confirmed by their disappearance after pre-incubation of the antibody with the specific peptide against which it was raised (Fig. 1d). Thus, our results demonstrate the presence of TRPV4 channels in migrating and non-migrating GnRH neurons.

To investigate whether TRPV4 channels were functional in the GN11 cell model, cells were loaded with fura-2AM and perfused with the selective chemical agonist, 4 α -phorbol 12,13 didecanoate (4 α -PDD) (1 μ M) (Watanabe *et al.* 2002;

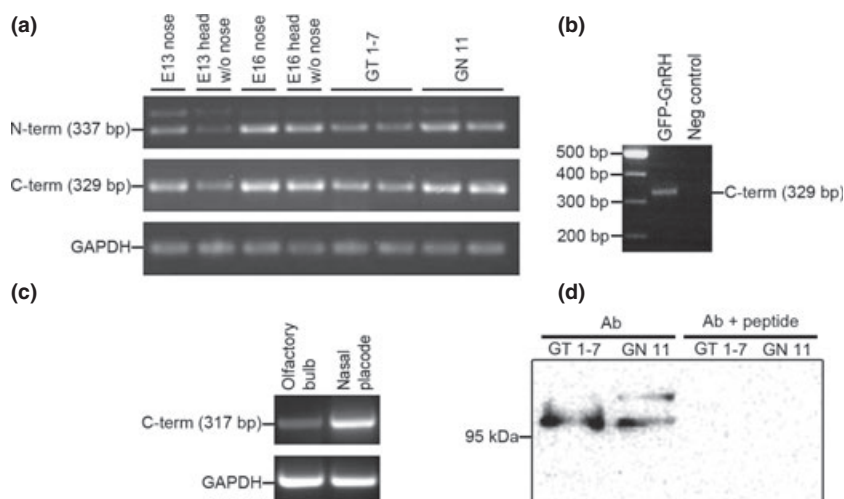


Fig. 1 Presence of TRPV4 during development and in gonadotropin-releasing hormone (GnRH) cell lines. (a) RT-PCR on mRNA extracted in mice embryos or in GT1–7 and GN11 cell lines. Primers amplified either the N-terminal or C-terminal region to assure specificity; E13 and E16 refer to the day at which RNA was extracted from embryos. (b) RT-PCR from sorted GFP⁺ cells from GFP-GnRH transgenic E17

embryos. (c) RT-PCR for TRPV4 transcript from the olfactory bulb and nasal placode of E16 rat embryos. (d) Western blotting using a specific antibody against TRPV4. Data are representative of at least three separate experiments on different preparations. For western blotting, similar data were obtained with a commercial antibody and an antibody raised in-house.

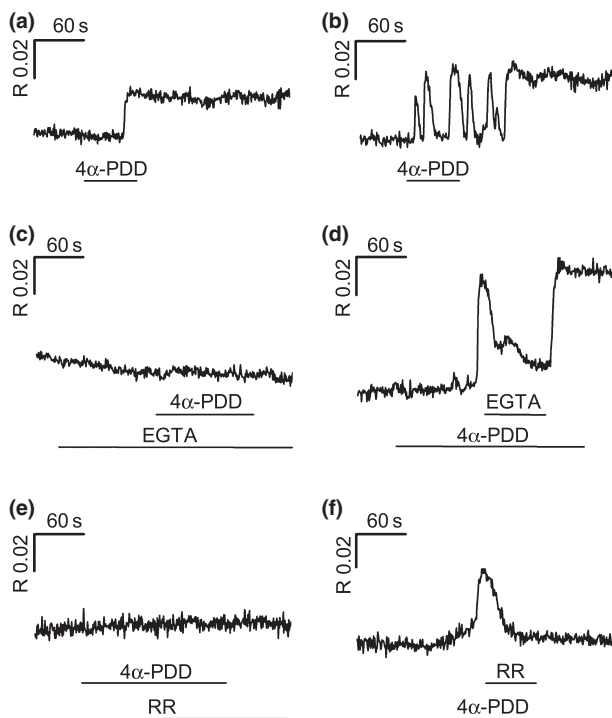


Fig. 2 TRPV4 elicits Ca^{2+} entry in GN11 cells. Drugs were added for the time indicated by the horizontal lines. (a and b) Different calcium responses elicited by 4α -PDD ($1 \mu\text{M}$); (c and d) effect of EGTA added before 4α -PDD or during a 4α -PDD-elicited response; (e and f) effect of ruthenium red ($1 \mu\text{M}$) added before 4α -PDD or during a 4α -PDD-elicited response. Traces are representative of typical responses. See text for number of cells analysed and percentage of responding cells.

Vriens *et al.* 2009). Analysis was then performed by choosing the entire cell diameter. Under these conditions, 39.5% (68/172) of cells responded with a sustained transient (Fig. 2a) and 5.2% (9/172) responded with oscillations (Fig. 2b). Performing experiments in the absence of extracellular calcium abolished responses to 4α -PDD (64/64; Fig. 2c), suggesting that influx through the plasma membrane was responsible for the calcium signal observed. Similar conclusions could be drawn in experiments where EGTA was added during the Ca^{2+} rise induced 4α -PDD (8/8; Fig. 2d). Pre-incubation of cells with ruthenium red ($1 \mu\text{M}$), a non-specific calcium channel blocker that also inhibits TRPV4 channels (Vriens *et al.* 2009), abolished responses to 4α -PDD (45/45; Fig. 2e). Last, when ruthenium red was added during the calcium response to 4α -PDD, the sustained response was also aborted (18/22; Fig. 2f).

These data taken together suggest therefore that TRPV4 channels are present and functional in GN11 cells.

Activation of TRPV4 inhibits chemotaxis in the Boyden's chamber

The feature that makes GN11 cells a unique experimental tool is their capacity to migrate, and this has been extensively

investigated by using the Boyden's chamber. In this assay, cells are placed in an upper chamber, while the lower chamber containing the chemotactic stimulus (1% FCS) is separated by a porous gelatin-coated membrane that needs to be crossed by cells. Surprisingly, the presence of 4α -PDD in the lower chamber reduced significantly the amount of migrating neurons (Fig. 3a). In detail, $10 \mu\text{M}$ 4α -PDD reduced migration by $87 \pm 1\%$ while $1 \mu\text{M}$ 4α -PDD reduced migration by $64 \pm 6\%$ compared with control. Ruthenium red ($1 \mu\text{M}$) was able to partially revert this effect and this was particularly evident when using $1 \mu\text{M}$ 4α -PDD (Fig. 3a). This effect was not because of cell toxicity, as treatment of cells for 3 h with 4α -PDD 1 or $10 \mu\text{M}$ did not result in significant toxicity ($93 \pm 9\%$ of control and $85 \pm 12\%$ of control; assessed by the 3-(4,5-dimethylthiazol-2-yl)-2,5-diphenyltetrazolium bromide assay). Longer treatments (24 h) yielded a modest toxicity, as would be expected from a calcium-entry channel activator ($79 \pm 3\%$ and $60 \pm 5\%$, respectively). To confirm the effect observed with 4α -PDD, we used a recently described 4α -phorbol analogue (4α -PDH) (Klausen *et al.* 2009) which also activates TRPV4. Indeed, also 4α -PDH inhibited chemotaxis of GN11 cells (data not shown; $10 \mu\text{M}$, $50 \pm 3\%$ of control). The phorbol ester phorbol-12-myristate-13-acetate (10 nM) was devoid of effect on migration, while arachidonic acid ($5 \mu\text{M}$) and 5,6-epoxyeicosatrienoic acid ($3 \mu\text{M}$), that have been proposed to be endogenous modulators of the TRPV4 channel (Watanabe *et al.* 2003), moderately inhibited migration ($74 \pm 3\%$ and $82 \pm 2\%$, respectively; Fig. 3b). From this pharmacological profile, it can be concluded that activation of TRPV4 channels leads to a decrease in microchemotaxis.

To strengthen the above observations, we decided to transflect GN11 cells with a bicistronic plasmid encoding for GFP and for *trpv4*, thereby over-expressing the channel. We then sorted by flow-cytometry fluorescent cells versus non-transfected neurons. Morphologically, over-expressing neurons appeared rounder in shape and displayed fewer lamellipodia-like structures (data not shown; see below for data on non-over-expressing cells). In the Boyden's chamber, over-expression of the channel resulted in reduced migration (Fig. 3c). As it has been shown that TRPV4 display constitutive activity at 37° , this reduced migration could have been anticipated. Even more interestingly, when microchemotaxis was inhibited by minute amounts of 4α -PDD (300 nM) which had only a minor effect on control cells (a decrease of 13.9%), over-expressing cells displayed a marked decrease (63.2%). From a pharmacological perspective, the higher sensitivity of these cells would be expected. Indeed, increasing the amount of receptors increases the possibility to form active complexes. These data therefore again indicate that TRPV4 channel activation leads to reduced microchemotaxis.

The observation that over-expression caused morphological changes led us to envisage that adhesion mechanisms

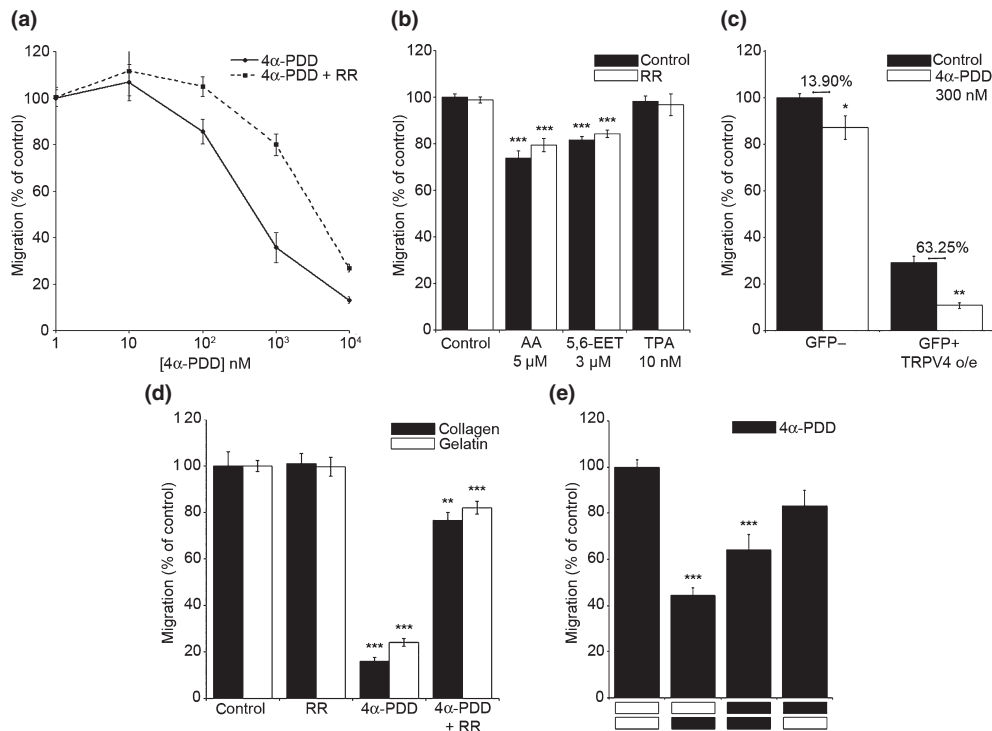


Fig. 3 Effect of 4α-PDD on microchemotaxis. (a) Concentration–response curve of 4α-PDD in the presence or absence of the non-specific TRPV4 inhibitor ruthenium red (RR; 1 μM). Values are mean ± SEM of 3–23 replicates from one to four experiments; (b) effect of arachidonic acid (AA), 5,6-epoxyeicosatrienoic acid or phorbol 12,13 myristate (TPA) on microchemotaxis in the presence or absence of ruthenium red. Values are mean ± SEM of 10–21 determinations in two to three separate experiments. (c) Effect of over-expression of TRPV4 channels on microchemotaxis. Cells were transfected with a bicistronic plasmid and were sorted for GFP fluo-

rescence. With this vector, GFP positive cells correspond to TRPV4-over-expressing (o/e) cells. Values are mean ± SEM of 5–17 determinations in two separate experiments. (d) Effect of different membrane coatings on microchemotaxis. Ruthenium red and 4α-PDD were used at 1 μM. Values are mean ± SEM of eight determinations in two separate experiments. (e) Effect of 4α-PDD 1 μM in the different compartments of the Boyden's chamber. Values are mean ± SEM of 13–15 replicates in three separate experiments. **p* < 0.05, ***p* < 0.01, ****p* < 0.001 compared with respective controls.

might be controlled by TRPV4 activation. Therefore, we performed microchemotaxis assays on either collagen- or gelatin-coated membranes. Cells migrated more across gelatin-coated compared with collagen-coated membranes (4960 ± 530 per well vs. 1500 ± 450 per well). Yet, no significant difference was observed in the percent of inhibition of migration induced by 4α-PDD (1 μM; Fig. 3d). It would therefore appear that if adhesion were involved, it is not substrate specific.

Two main reasons could explain the inhibitory effect observed with the activators of TRPV4: 4α-PDD could act as a chemorepulsant or could reduce the motor performance of neurons. To investigate this, we decided to place the compound either only in the bottom chamber, only in the top chamber or collapse the gradient and place equal concentrations of compound in both chambers. As shown in Fig. 3(e), migration was least when 4α-PDD was placed only in the bottom chamber while it was higher when it was placed directly with cells but not together with the chemotactic stimulus. This suggests that it is likely that activation of

TRPV4 acts as a repulsive stimulus. Yet, when 4α-PDD was added just to the upper chamber, total migrated cells were lower than control, supporting a possible role of TRPV4 also on the speed of movement.

Activation of TRPV4 hampers migration also in other *in vitro* models

While the Boyden's chamber is a validated model for microchemotaxis, it can be argued that migration is rather more complex and therefore we decided to investigate the role played by TRPV4 channels also in other models. First, we performed wound healing assays. In this assay, a scratch is performed on a sub-confluent monolayer of cells and the re-population of the region is monitored with time. Control GN11 cells are able to repopulate the scratch area within 16–18 h. In the presence of ruthenium red (1 μM), there is no difference compared with control in the time required to re-colonize the scratch area. On the other hand, in the presence of 4α-PDD (1 μM) cells are unable to make any substantial progress in the same time-frame, and this effect

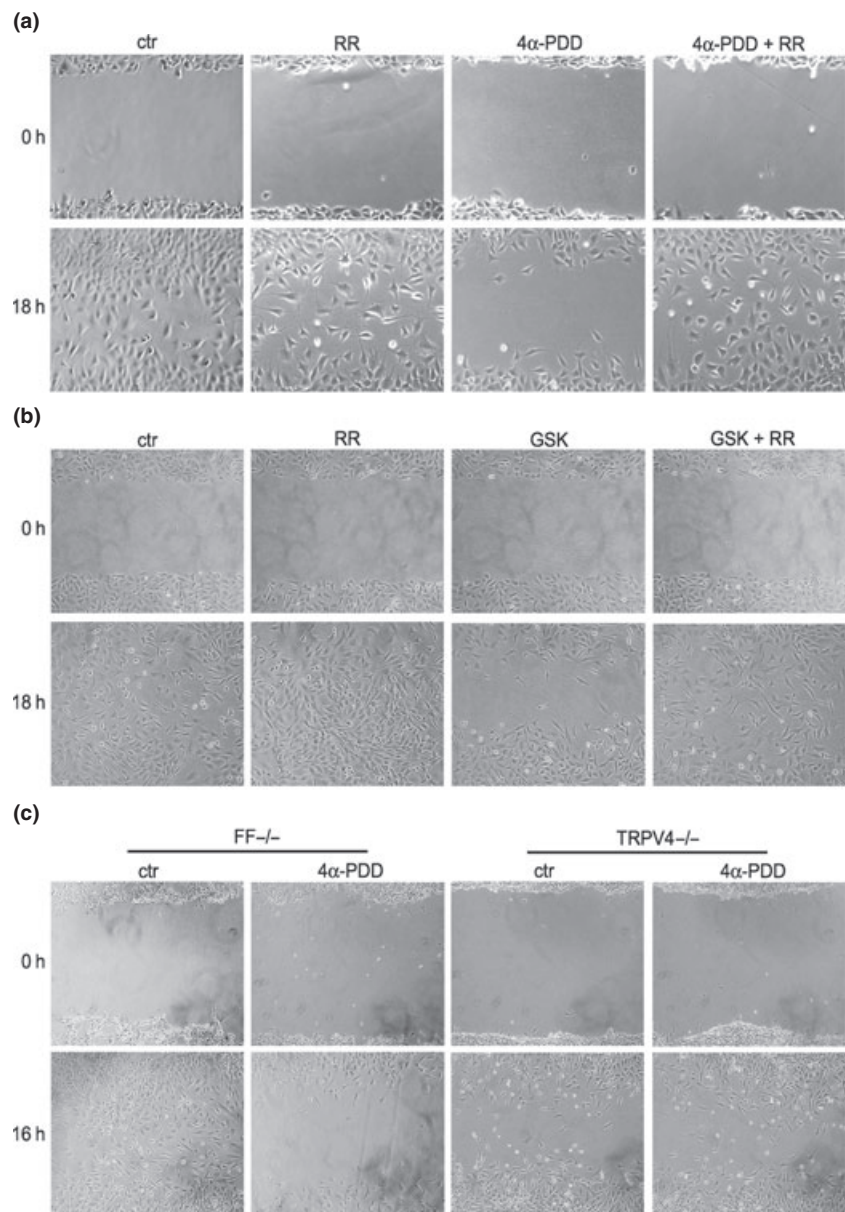


Fig. 4 Effect of 4 α -PDD (panel a) or GSK1016790A (GSK) (panel b) on wound healing in GN11 cells. In panel (c), experiments were conducted with cells in which TRPV4 expression was decreased via siRNA (TRPV4 $^{-/-}$). As a control, siRNAs specific for the firefly gene (FF) were used. The following concentrations were used: ruthenium red (RR) 1 μ M, 4 α -PDD 1 μ M, GSK 10 nM. Photos are representative of at least three experiments and were taken at 16/18 h.

can be reverted by the co-incubation with ruthenium red (Fig. 4a). It has been shown that GSK1016790A is another activator of TRPV4 and it is structurally distinct from PDD and PDH as it is not a phorbol ester (Thorneloe *et al.* 2008). As a further control, we therefore analysed the effect of this compound on the wound assay. 3-(4,5-Dimethylthiazol-2-yl)-2,5-diphenyltetrazolium bromide assays suggested that GSK1016790A is relatively toxic to cells (treatment of cells for 24 h with 100 nM GSK1016790A yielded a survival of $35 \pm 1\%$ of cells, interestingly this effect was reverted by ruthenium red), and therefore lower concentrations were used (10 nM; survival after 16 h treatment was $87 \pm 3\%$ of control). As expected, also this compound abolished the ability of GN11 cells to

re-populate the scratch area (Fig. 4b). As a final control, we investigated whether, in this model, *trpv4* gene knockdown by siRNA would change migratory behaviour. Efficiency of knockdown was 75% as assessed by real-time PCR. Cells with depleted levels of *trpv4* were able to yield scratch closure, but this effect was no longer sensitive to 4 α -PDD.

Last, we studied the effect of 4 α -PDD in a 3D model of cell migration, represented by the collagen gel assay. In this assay, when 4 α -PDD was present in the extracellular space, GN11 cells were unable to move out of the cell aggregates into the collagen matrix (Fig. 5).

TRPV4 channels therefore alter migration via influencing behaviours that are common to a number of different models, and do not pertain just to chemotaxis.

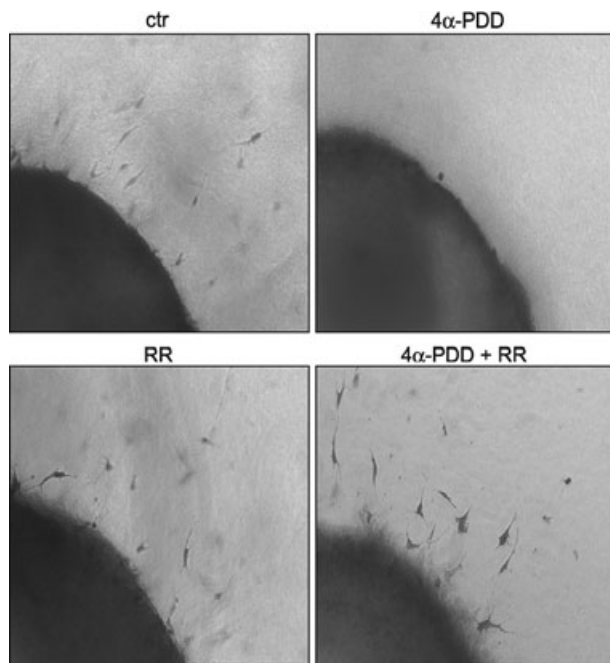


Fig. 5 Effect of 4α -PDD on collagen aggregates. Photos are representative of four experiments and were collected at 48 h. The following concentrations were used: ruthenium red (RR) $1\ \mu\text{M}$, 4α -PDD $1\ \mu\text{M}$.

4α -PDD affects 2-D migration of GN11 cells

As chemotaxis was not the only affected cell function, we hypothesized that 2D migration in the absence of gradients could also be affected. To assess the role of TRPV4 channels on GN11 cell migration, we therefore compared cell morphology changes (circularity) and cell motion parameters (speed and direction changes) in control conditions and in the presence of 4α -PDD in time-lapse experiments.

Figure 6(a) shows a time-lapse series of a migrating cell initially bathed in control medium (30 and 150 min) and then in a medium containing vehicle alone (290 and 440 min) while Fig. 6(b) shows the entire trajectory of the cell. Neither change in cell circularity nor in the rate of migration was observed in response to medium perfusion. The mean values of the speed of migration v for this cell, in control condition and vehicle, were $1.02 \pm 0.09\ \mu\text{M}/\text{min}$ and $1.00 \pm 0.09\ \mu\text{M}/\text{min}$, respectively.

Figure 6(c) shows a time-lapse series of a migrating cell initially bathed in control medium (30 and 150 min) and then in medium containing 4α -PDD ($1\ \mu\text{M}$). In this case, soon after addition of the drug the cell retracted its protrusions and assumed a more spherical shape. About 30% of the cells treated with 4α -PDD underwent this marked morphological change. It should be noted that such behaviour has also been occasionally observed in unstimulated migrating cells. Figure 6(d) shows the trajectory of the depicted cell obtained in control medium (black line) or in the presence of 4α -PDD (red line). 4α -PDD induced a significant decrease of the rate

of migration, as evidenced by the comparison between the mean value of v of $1.39 \pm 0.08\ \mu\text{M}/\text{min}$, obtained in control medium, and of $0.85 \pm 0.11\ \mu\text{M}/\text{min}$ obtained in the presence of the TRPV4 agonist.

The effect of the agonist on cell morphology in the cells analysed is resumed in Fig. 7(a) that shows the cell average circularity plotted as a function of time. The black curve was obtained from cells ($n = 7$) in which, at the time indicated by the arrow, vehicle alone was perfused, whereas the red curve is relative to cells ($n = 8$) stimulated with 4α -PDD. The mean percentage change of speed induced by vehicle or 4α -PDD is summarized in Fig. 7(b). The TRPV4 agonist significantly decreased the rate of migration to $62.0 \pm 4.7\%$ of the control rate ($p < 0.01$). These experiments did not take into account cells that did not present a migratory phenotype in the course of the first 60 min of analysis. As mentioned below, these latter cells can be identified morphologically as being with stellate morphology with several thin protrusions or large, flat and polygonal (Fig. 8(a)). This effect of 4α -PDD on motility is supported by Boyden's experiments (Fig. 3d).

Finally, we analysed the frequency distributions of the instantaneous direction change angles $\Delta\phi$. Figure 7(c) represents the normalized average distributions obtained from cells moving in control medium (black curve) and in the presence of the vehicle (green curve). Curves are symmetrically centred at around 0° and nearly indistinguishable. On the contrary, as shown by the comparisons of the traces of Fig. 7(d), the presence of the agonist produced a lower occurrence of angles around 0° and $\pm 180^\circ$ and increased the frequency of angles around $\pm 90^\circ$. This observed loss of cell directionality indicates that TRPV4 channels play a fundamental role in the maintenance of GN11 cell polarity and motion persistence.

A detailed inspection of the time-lapse experiments revealed that most migrating GN11 cells are polarized cells, with a spindle or triangle-shape morphology with a broad lamellipodial protrusion [Fig. 8a, panel (i)]. In addition, cells with stellate morphology with several thin protrusions with active tips and stationary large flat polygonal cells were also observed. Upon addition of 4α -PDD, the first two cell types responded with a morphological change, while the latter did not. We therefore decided to analyse specifically the effect of 4α -PDD on this morphological change. In cells stimulated with 4α -PDD, this event started with the detachment of the leading lamellipodium, as shown in the time-lapse series of Fig. 8(a) (white arrow). On the contrary, stellate cells retracted almost simultaneously all their protrusions. In a different set of cells, we analysed the immuno-localization of TRPV4. In cells sharing the spindle or triangle-shape morphology, TRPV4-specific staining appeared localized at the tip of lamellipodial structures [Fig. 8a, panel (vi)], while in stellate cells staining was present at most tips of protrusions. Flat, stationary polygonal cells (which did not

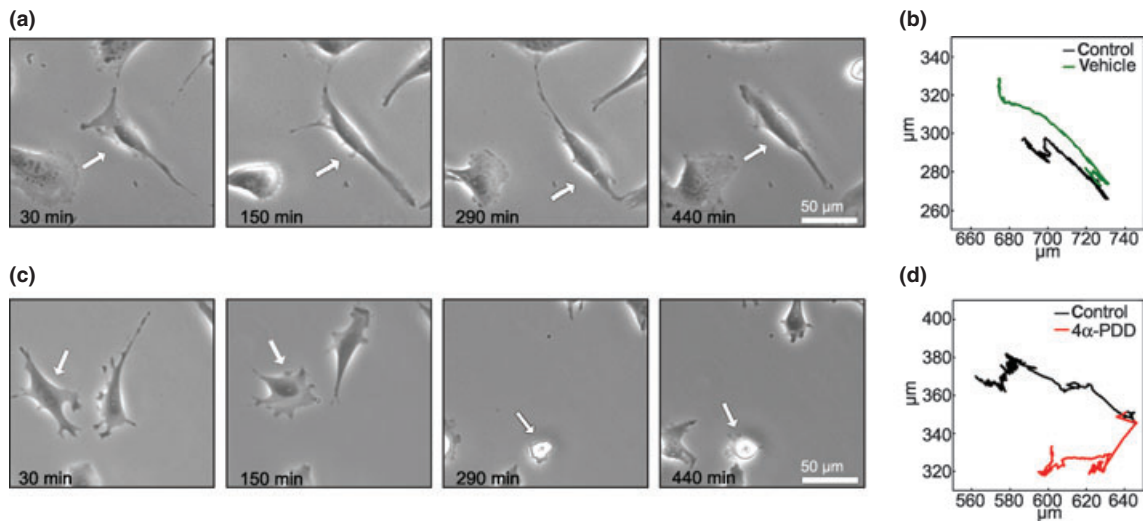
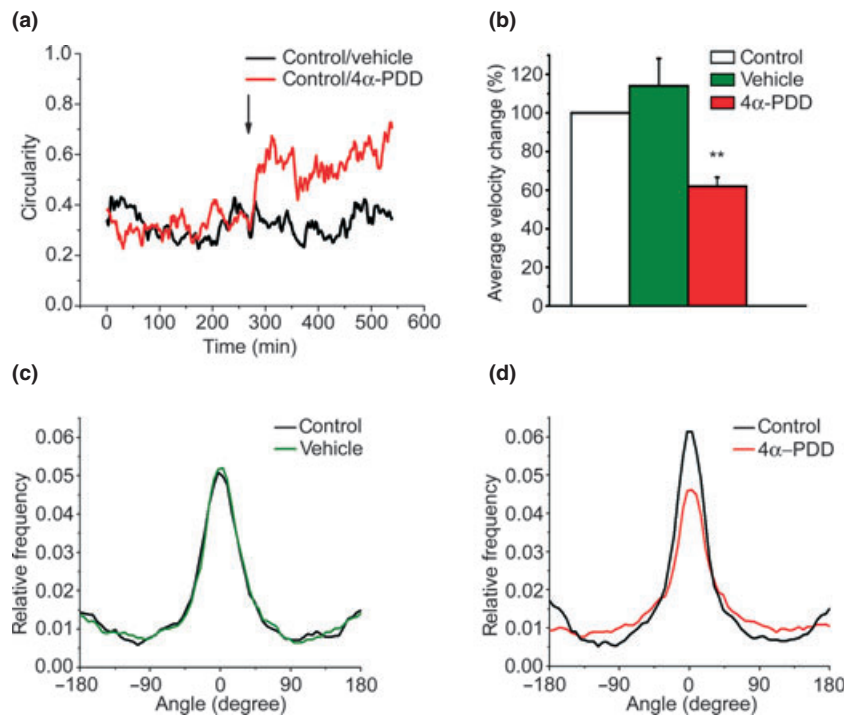


Fig. 6 Time-lapse of cell trajectories. Representative example of trajectory and shape of control (a and b) and treated (c and d) cells in time-lapse analysis. Figures (b) and (d) refer to cells depicted in panels (a) and (c), respectively. See Fig. 7 for cumulative data on all cells analysed.

Fig. 7 Cumulative data on the effect of TRPV4 on cell morphology and migration. (a) Average cell circularity plotted as function of the time. Cells were initially maintained in control medium. Arrow indicates the beginning of vehicle (black trace) or 4 α -PDD (red trace) perfusion. (b) Comparison of percent change in average speed measured in cells bathed in vehicle (green bar) and 4 α -PDD (red bar). ** $p < 0.01$ vs. control. (c and d) Comparison of normalized histograms of the average frequency distribution of direction changes $\Delta\phi$. (c) Compares the distributions of angles obtained when cells were initially bathed in control medium (black trace) and then in the presence of vehicle (green). Likewise (d) shows the distribution of angles obtained in control medium (black) and in the presence of 4 α -PDD (red). Data refer to seven control cells and eight treated cells chosen on the basis of morphology (see Fig. 8) and initial motility in the first hour.



respond to 4 α -PDD with morphological changes; see before) presented hardly any specific TRPV4 staining. Last, we also analysed in time and space the calcium-increase elicited by 4 α -PDD. Calcium was measured either by Fura-2 (Fig. 8b; re-analysing the experiments from Fig. 2a placing regions of interest at the margin of cells that appeared to have a polarized morphology) or by the NT-XL probe (a ratiometric fluorescence resonance energy transfer (FRET)-based probe; Fig. 8c) in confocal microscopy. With both strategies we

could observe that calcium signals elicited by 4 α -PDD were more pronounced at the leading edge of cells, suggesting that this region is the primary site of Ca²⁺ entry.

Discussion

In this article, we have shown that *trpv4* channels are present and functional in an immortalized cell line of GnRH-secreting neurons and that the localization of this channel

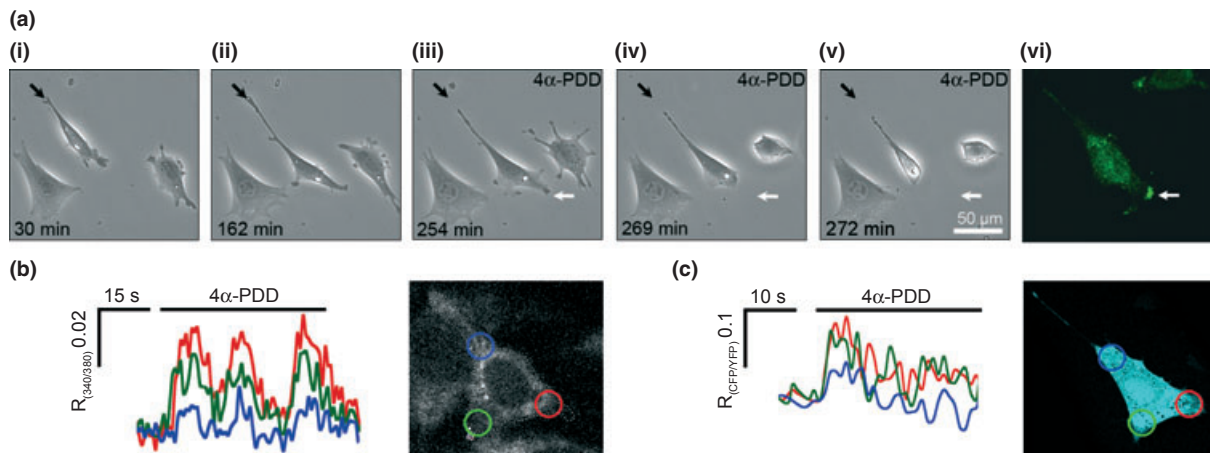


Fig. 8 Correlation of TRPV4 localization, calcium signals elicited by 4 α -PDD and lamellipodia retraction. (a, panel i–v). A field of cells in which all the GN11 cell types are represented and their morphological response to 4 α -PDD (1 μ M); (vi) immunolocalization of TRPV4 channels in a spindle-shape cell (representative cell of about 200 cells analysed from three independent experiments with similar staining patterns). (b) Calcium signals elicited by 4 α -PDD and analysed from

selected regions of interest as recorded by fura-2AM fluorescence microscopy (representative trace of 26 cells analysed from three independent experiments with similar results); (c) calcium signals elicited by 4 α -PDD and analysed from selected regions of interest as recorded by the NT-XL probe in fluorescence confocal microscopy (representative trace of 16 cells analysed from four independent experiments with similar results).

appears polarized and enriched in lamellipodial structures. This is confirmed from Ca^{2+} measurements which show that Ca^{2+} rises are not uniformly distributed throughout the cell. The activation of these channels leads to a retraction of the lamellipodia and to a decrease in migratory behaviour as assessed in three different models and demonstrated both pharmacologically and with molecular tools. Furthermore, live-imaging experiments showed that, in the presence of 4 α -PDD, cells migrate slower and in a more random manner.

The link between calcium and migration, albeit strong, has never been elucidated fully. A pivotal paper by Brundage and Fay (Brundage *et al.* 1991) demonstrated that in eosinophils, following a chemotactic stimulus, a calcium gradient exists and that calcium is highest at the rear end of cells. It has then been elucidated and accepted that Ca^{2+} increases, mostly mediated by stretch-activated channels, allow for detachment of the rear cell margin to allow for progression forward of the cell (Lee *et al.* 1999). Yet, calcium channels are present also at the leading edge and lamellae and Ca^{2+} -decoding machinery is also present in these regions, suggesting that this ion must also play a role in this region. Recently, it has been shown that, in leading lamellae, small, localized calcium bursts (flickers) are present and coordinate ‘cell steering’. In fibroblasts, these flickers appear to be mediated by the opening of TRPM7 (Wei *et al.* 2009). In an artificial setting, that is, over-expressing TRPC1 cells, careful analysis has led to the proposal that TRP mechanoreceptors may be present in the lamellipodium and determine polarity and direct cell migration (Fabian *et al.* 2008). In this context, we now report that TRPV4 are present at the leading edge of cells and their strong activation leads to cell retraction. It is

important to note, that, although novel, the observation in this article overlaps with observations by others on the growth cone (Henley and Poo 2004; Henley *et al.* 2004). For example, it has been shown that Slit-2 induces a calcium wave from growth cone to soma which leads to reversal of neuronal migration (Guan *et al.* 2007).

The mechanism by which this occurs is at present unclear, although it has been suggested by others that TRPV4 displays a functional interaction with microfilaments and the cytoskeleton (Goswami *et al.* 2010), and this might provide a mechanism by which the leading edge might change shape. On the other hand, it has also been shown that activation of TRPV4 channels induce endothelial cell re-orientation via an indirect link to integrins, which then mediate adhesion and cell remodelling (Thodeti *et al.* 2009). Indeed, this last observation would explain the retraction observed in our experiments. Similarly, the possibility that Ca^{2+} entry through TRPV4 channels coordinates RhoA activity cannot be ruled out (Guan *et al.* 2007).

As TRPV4 channels are present in the brain during development, it would be exciting to speculate that these channels play a role in determining neuronal migration in cells other than GnRH neurons. If so, given the multiple activation pathways for this channel (Watanabe *et al.* 2003), it would remain to be established what are the physiological stimuli that would regulate their activation.

Acknowledgements

We thank Prof. Giovanni Appendino for providing 4 α -PDH. This work was supported by the Regione Piemonte (Ricerca Sanitaria

Finalizzata 2008, 2008bis and 2009), by MIUR (Prin 2007 to AAG) and by the Fondazione Cariplo (Ricerca Biomedica 2008) to AAG. We thank Ornella Mesenzani and Fani Memi for technical support with RT-PCR experiments.

Supporting Information

Additional supporting information may be found in the online version of this article:

Appendix S1. Detailed methods.

As a service to our authors and readers, this journal provides supporting information supplied by the authors. Such materials are peer-reviewed and may be re-organized for online delivery, but are not copy-edited or typeset. Technical support issues arising from supporting information (other than missing files) should be addressed to the authors.

References

- Berridge M. J. (2001) The versatility and complexity of calcium signalling. *Novartis Found. Symp.* **239**, 52–64; discussion 64–57, 150–159.
- Brundage R. A., Fogarty K. E., Tuft R. A. and Fay F. S. (1991) Calcium gradients underlying polarization and chemotaxis of eosinophils. *Science* **254**, 703–706.
- Cariboni A., Hickok J., Rakic S., Andrews W., Maggi R., Tischkau S. and Parnavelas J. G. (2007) Neuropilins and their ligands are important in the migration of gonadotropin-releasing hormone neurons. *J. Neurosci.* **27**, 2387–2395.
- Clapham D. E., Montell C., Schultz G. and Julius D. (2003) International Union of Pharmacology. XLIII. Compendium of voltage-gated ion channels: transient receptor potential channels. *Pharmacol. Rev.* **55**, 591–596.
- Fabian A., Fortmann T., Dieterich P., Riethmuller C., Schon P., Mally S., Nilius B. and Schwab A. (2008) TRPC1 channels regulate directionality of migrating cells. *Pflugers Arch.* **457**, 475–484.
- Goswami C., Kuhn J., Heppenstall P. A. and Hucho T. (2010) Importance of non-selective cation channel TRPV4 interaction with cytoskeleton and their reciprocal regulations in cultured cells. *PLoS ONE* **5**, e11654.
- Guan C. B., Xu H. T., Jin M., Yuan X. B. and Poo M. M. (2007) Long-range Ca²⁺ signaling from growth cone to soma mediates reversal of neuronal migration induced by slit-2. *Cell* **129**, 385–395.
- Henley J. and Poo M. M. (2004) Guiding neuronal growth cones using Ca²⁺ signals. *Trends Cell Biol.* **14**, 320–330.
- Henley J. R., Huang K. H., Wang D. and Poo M. M. (2004) Calcium mediates bidirectional growth cone turning induced by myelin-associated glycoprotein. *Neuron* **44**, 909–916.
- Klausen T. K., Pagani A., Minassi A., Ech-Chahad A., Prenen J., Owsianik G., Hoffmann E. K., Pedersen S. F., Appendino G. and Nilius B. (2009) Modulation of the transient receptor potential vanilloid channel TRPV4 by 4 α -phorbol esters: a structure-activity study. *J. Med. Chem.* **52**, 2933–2939.
- Lee J., Ishihara A., Oxford G., Johnson B. and Jacobson K. (1999) Regulation of cell movement is mediated by stretch-activated calcium channels. *Nature* **400**, 382–386.
- Mank M., Reiff D. F., Heim N., Friedrich M. W., Borst A. and Griesbeck O. (2006) A FRET-based calcium biosensor with fast signal kinetics and high fluorescence change. *Biophys. J.* **90**, 1790–1796.
- Monet M., Lehen'kyi V., Gackiere F. *et al.* (2010) Role of cationic channel TRPV2 in promoting prostate cancer migration and progression to androgen resistance. *Cancer Res.* **70**, 1225–1235.
- Nilius B. and Owsianik G. (2010) Channelopathies converge on TRPV4. *Nat. Genet.* **42**, 98–100.
- Nilius B., Owsianik G., Voets T. and Peters J. A. (2007) Transient receptor potential cation channels in disease. *Physiol. Rev.* **87**, 165–217.
- Orso F., Jager R., Calogero R. A., Schorle H., Sismondi P., De Bortoli M. and Taverna D. (2009) AP-2 α regulates migration of GN-11 neurons via a specific genetic programme involving the Axl receptor tyrosine kinase. *BMC Biol.* **7**, 25.
- Rock M. J., Prenen J., Funari V. A. *et al.* (2008) Gain-of-function mutations in TRPV4 cause autosomal dominant brachyolmia. *Nat. Genet.* **40**, 999–1003.
- Schwanzel-Fukuda M. and Pfaff D. W. (1989) Origin of luteinizing hormone-releasing hormone neurons. *Nature* **338**, 161–164.
- Thodeti C. K., Matthews B., Ravi A., Mammoto A., Ghosh K., Bracha A. L. and Ingber D. E. (2009) TRPV4 channels mediate cyclic strain-induced endothelial cell reorientation through integrin-to-integrin signaling. *Circ. Res.* **104**, 1123–1130.
- Thorneloe K. S., Sulpizio A. C., Lin Z. *et al.* (2008) N-((1S)-1-[[4-((2S)-2-[[[(2,4-dichlorophenyl)sulfonyl]amino]-3-hydroxypropyl]-1-piperazinyl]carbonyl]-3-methylbutyl)-1-benzothiophene-2-carboxamide (GSK1016790A), a novel and potent transient receptor potential vanilloid 4 channel agonist induces urinary bladder contraction and hyperactivity: part I. *J. Pharmacol. Exp. Ther.* **326**, 432–442.
- Toba Y., Pakiam J. G. and Wray S. (2005) Voltage-gated calcium channels in developing GnRH-1 neuronal system in the mouse. *Eur. J. Neurosci.* **22**, 79–92.
- Tobet S. A. and Schwarting G. A. (2006) Minireview: recent progress in gonadotropin-releasing hormone neuronal migration. *Endocrinology* **147**, 1159–1165.
- Venekens R., Owsianik G. and Nilius B. (2008) Vanilloid transient receptor potential cation channels: an overview. *Curr. Pharm. Des.* **14**, 18–31.
- Vriens J., Appendino G. and Nilius B. (2009) Pharmacology of vanilloid transient receptor potential cation channels. *Mol. Pharmacol.* **75**, 1262–1279.
- Waning J., Vriens J., Owsianik G., Stuwe L., Mally S., Fabian A., Fripiat C., Nilius B. and Schwab A. (2007) A novel function of capsaicin-sensitive TRPV1 channels: involvement in cell migration. *Cell Calcium* **42**, 17–25.
- Watanabe H., Davis J. B., Smart D. *et al.* (2002) Activation of TRPV4 channels (hVRL-2/mTRP12) by phorbol derivatives. *J. Biol. Chem.* **277**, 13569–13577.
- Watanabe H., Vriens J., Prenen J., Droogmans G., Voets T. and Nilius B. (2003) Anandamide and arachidonic acid use epoxyeicosatrienoic acids to activate TRPV4 channels. *Nature* **424**, 434–438.
- Wei C., Wang X., Chen M., Ouyang K., Song L. S. and Cheng H. (2009) Calcium flickers steer cell migration. *Nature* **457**, 901–905.
- Wray S., Nieburgs A. and Elkabes S. (1989) Spatiotemporal cell expression of luteinizing hormone-releasing hormone in the prenatal mouse: evidence for an embryonic origin in the olfactory placode. *Brain Res. Dev. Brain Res.* **46**, 309–318.
- Zaninetti R., Tacchi S., Erriquez J., Distasi C., Maggi R., Cariboni A., Condorelli F., Canonico P. L. and Genazzani A. A. (2008) Calcineurin primes immature gonadotropin-releasing hormone-secreting neuroendocrine cells for migration. *Mol. Endocrinol.* **22**, 729–736.
- Zheng J. Q. and Poo M. M. (2007) Calcium signaling in neuronal motility. *Annu. Rev. Cell Dev. Biol.* **23**, 375–404.